EXPERIMENTAL INVESTIGATIONS OF THE PMMA BONE CEMENT DISTRIBUTION INSIDE A MODEL OF LUMBAR VERTEBRAE

Artur Bonik[1]* (iD), Zbigniew Tyfa[2] (iD),
Lechosław F. Ciupik[1] (iD), Krzysztof Sobczak[2] (iD),
Agnieszka Kierzkowska[1] (iD), Damian Obidowski[2] (iD),
Dariusz Witkowski[2] (iD), Tomasz Pałczyński[2] (iD),
Marcin Elgalal[3] (iD), Piotr Komorowski[3] (iD),
Edward Słoński[1] (iD), Krzysztof Jóźwik[2] (iD),
Bogdan Walkowiak[3] (iD)

[1] LfC Ltd. Medical, 41 Kożuchowska St.,
65-364 Zielona Góra, Poland
[2] Lodz University of Technology,
Faculty of Mechanical Engineering,
Institute of Turbomachinery,
Wólczańska 219/223 St., 90-924 Łódź, Poland
[3] Molecular and Nanostructural Biophysics
Laboratory, BioNanoPark Laboratories,
114/116 Dubois St., 93-465 Lodz, Poland
*e-mail: arturbonik@gmail.com

Abstract

The use of bone cement in procedures such as vertebroplasty and kyphoplasty can reduce pain and mechanically support the spine. This study aimed to evaluate whether air entrapped within bone cement affected its distribution in a vertebral body model. The study included 3D printed anatomical models of vertebrae together with their internal trabecular structure. Aeration was achieved by mixing the bone cement using three different altered procedures, whilst the control sample was prepared according to the manufacturer's instructions. The further two samples were prepared by reducing or increasing the number of cycles required to mix the bone cement. A test rig was used to administer the prepared bone cement and introduce it into the vertebral model. Each time the injection was stopped when either the cement started to flow out of the vertebral model or when the entire cement volume was administered. The computer tomography (CT) scanning was performed to evaluate aerification and its influence on the bone cement distribution in each of the patient-specific models. The large number of small pores visible within the cement, especially in the cannula vicinity, indicated that the cement should not be treated as a homogenous liquid. These results suggest that a high level of aerification can influence the further cement distribution.

***Keywords:** percutaneous vertebroplasty, osteoporotic spinal fractures, spinal cement injection, cement distribution, bone cement preparation*

Introduction

Osteoporosis causes a decrease in bone mass and a degeneration of the bone tissue microarchitecture in the spine section [1]. Compression and osteoporotic bone fractures are characteristic of osteoporosis [2]. Most compression and osteoporotic fractures are fixed within several months from the first complaint occurrence. During this period, conservative healing methods are used, such as massages, pharmacological treatments, and limiting movement [3]. In a situation where the pain caused by osteoporotic compression fractures [4] or vertebral body cancerous changes cannot be endured any longer, it is necessary to support the spine mechanically with vertebroplasty, kyphoplasty and/or by enhancing the spinal column with implants [5].

In mini-invasive enhancing procedures [6] such as vertebroplasty and kyphoplasty, the bone cement is injected with a needle into the damaged vertebrae under radiological supervision. Polymethylmethacrylate (PMMA) is used most frequently for this purpose [7]. A small amount of cement, ranging from 2.5 to 4.5 ml, is placed in the vertebrae, which is enough to restore its biomechanical parameters, as shown in numerous research results [8-9]. To avoid complications, the filling procedure is stopped when the cement approaches the defect, the anatomical orifice, or when the cement leaks out beyond the cortical bone of the vertebra in any direction [10].

Previous investigations [12] show that PMMA-based cement can be characterized by a variable level of aerification [13], which is strictly related to the cement mixing process. Aerification and compressibility can change the general material flow dynamics, especially the injection speed. The cement tenacity grows as a result of the components chemical reactions during the polymerization process, which increases the flow resistance.

The cement injection into the bone structure should be made during its optimal tenacity [14]. When the cement is applied at the too low tenacity, it can lead to uncontrollable liquefaction. If the cement tenacity is too high, the flow resistance can hinder its further propagation in the bone. As a result, not only will the intended outcome not be achieved [15], but the patient's health can be at serious risk [17]. The most common complication that occurs in the procedure is the cement leakage, defined as the bone cement escape beyond the vertebral body [16-18]. Most leaks are local and asymptomatic [19]. Otiz [20] divides complications related to the procedure of enhancing the vertebrae with bone cement into two groups. The first group covers local complications, consisting in damages and changes connected directly to the vertebrae surrounding. The second group is systemic complications which influence the systems and organs proper functioning. The majority of risks associated with transdermic vertebroplasty can be minimalized by actions that prevent leaks, such as controlling the medium distribution.

The main objective of these investigations was to analyze via CT scans the influence of cement aerification on its distribution in the vertebral body model developed and 3D printed by the authors. During the last decade, PMMA-based cements and their features have been widely discussed. The research was mainly focused on creating new cements and composites, improving mechanical features [21], improving biological response [22], rheological and mechanical features of cement materials [23-27]. However, no research has been reported on the cement injection and its distribution in an anatomic model of vertebrae, built with the 3D printing technology. This indicates the novelty of the subject presented in this work. In order to achieve the intended purpose, experimental studies were carried out, requiring the preparation of suitable models and the use of several sets of biomedical cements.

Methodology

The conducted investigations composed of four phases. In the first phase, a digital reconstruction of the lumbar vertebra with osteoporotic changes was prepared by the computer microtomography based on anatomic medical data. The obtained model was segmented and processed digitally in order to be printed in the 3D technology. During the second phase, a precise physical model with an internal structure was printed with the 3D printer (Ultimaker 3, manufactured by Ultimaker B.V., The Netherlands). The next phase was to prepare the properly aerified bone cement and to inject it into the previously prepared models of vertebrae. The last phase consisted in an inspection of the bone cement distribution in the filled model with the computer microtomography.

Reconstruction

The anatomic digital data of the lumbar vertebra with osteoporotic changes, saved as a DICOM file (Digital Imaging and Communications in Medicine) were reconstructed and segmented with the Mimics Medical™ software developed by the Materialise company. Next, the data from the segmentation were subjected to digital processing. The model mesh was optimized with respect to the scope of the print, removing the too fine or loose elements. The back part was also removed, as it was irrelevant in the cement distribution analysis, leaving thus the vertebra alone. The model was modified by implementing a mechanical connection that ensured the same entry point into the vertebra and a repeatable injection point. The prepared 3D digital model was exported to a STL file, which allowed it to be imported and printed. FIG. 1 shows a view of the model with planes indicating its cross-sections, as well as the selected internal micro-architecture.

Physical 3D model preparation

The physical model of vertebrae with their internal structure was printed with the Ultimaker 3 printer (Ultimaker B.V., the Netherlands) in the FDM technology (Fused Deposition Modelling) which is one of the most often used additive manufacturing technologies of wires made of PLA (polylactic acid).

The vertebra digital model in a STL format was imported to the Ultimaker Cura 3D software. The printing parameters were selected from available options, such as a layer thickness, a filling structure, and a head speed. Next, the position and orientation of the model, which needed some support pillars, were fixed. This process was repeated several times until the acceptable configuration of the pillars was achieved, which would allow the model to be printed with the internal structure backed by the supporting material. A Gcode machine code was generated for the model to allow its printing on the 3D printer. The printer was equipped with two printing heads to print the model in two types of material. The elements of the vertebra model were printed in PLA, whereas the supporting elements were printed in water-soluble PVA. After printing, the elements were immersed in water for 24 h to dissolve the supporting material. Then, after rinsing, the model was left for 24 h to dry. Next, the prepared models were used in further investigations.

Experimental investigations

The test rig, configured for previous investigations where it had been verified as accurate and repeatable, was used [12]. A scheme of testing is presented in FIG. 2. The whole experimental system consisted of four main parts [12]. The first one, the Legato™210 infusion pump, was used as a cement flow generator, maintaining a constant given speed of the syringe plunger. A 10 cm^3 capacity syringe made of acrylic glass was fixed in the infusion pump. The second part was an acrylic glass cannula connected to a pressure transducer via a pressure connector. The third piece, a glass cannula, served as a mechanical connection of the flow channel and the solid 3D vertebra model. Both cannulas had the same 3.0 mm internal diameter and were connected collinearly to minimize the flow disruption. Furthermore, they were transparent so as to observe the distribution of the flowing medium and to pinpoint the moment the cement began to flow into the vertebrae. Both cannulas were 72 mm long and the distance between the pressure tap and the model was 62 mm.
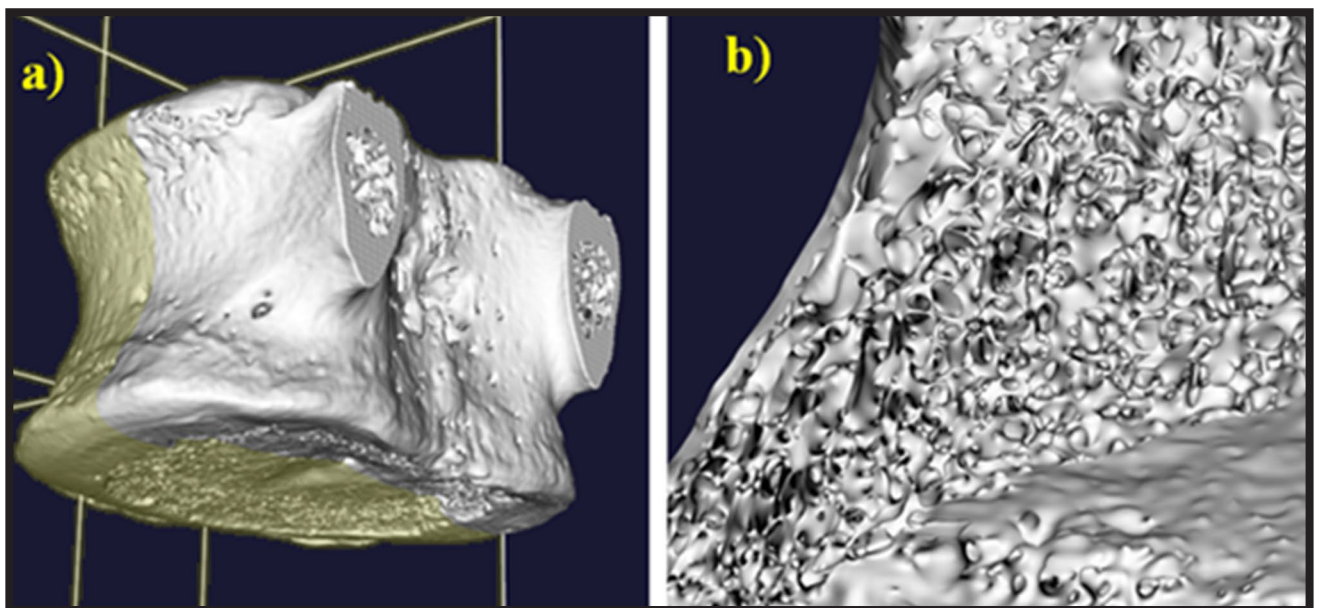
FIG. 1. View of a vertebra model: a) with planes indicating its cross-sections; b) visualization of the internal micro-architecture.
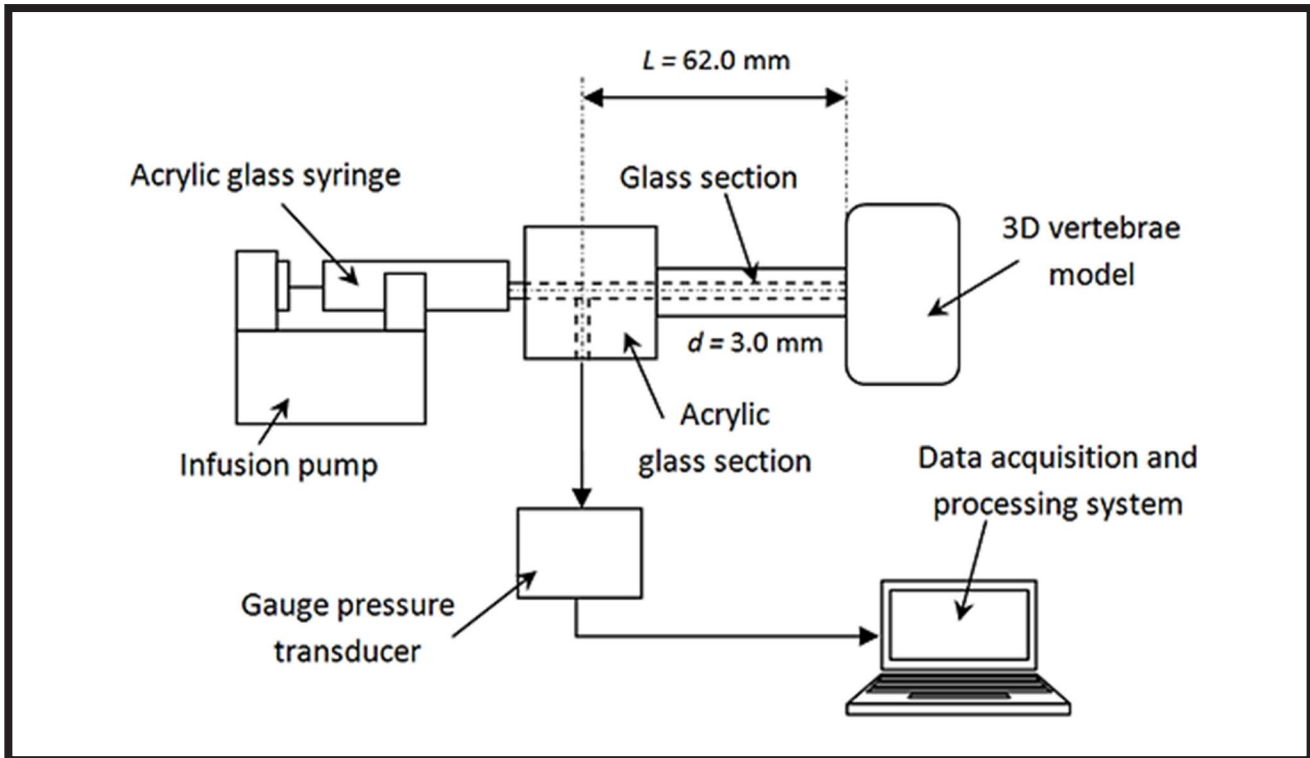
FIG. 2. Scheme of the test rig for investigations of the injection and distribution of bone cements in the 3D vertebra model.

Three models P1, P2, and P3 used in each trial were printed under the same conditions, from the same material, using the same 3D printer. The models resembled vertebrae with a weakened structure which needed to be supported by an implant, the bone or the cement, or both. In our case, the 3D printing of the bone structure was based on medical images, so we could claim that it correctly reproduced the porous bone structure in accordance with the Wolf's law. The change in bone density [28] affected the flow resistance of the cement inside the models. At the beginning of the tests, the flow channels in the model were filled with air. The glass cannula was inserted into a hole drilled in the vertebrae model. The tolerance of the cannula position was ±1.8 mm horizontally and ±0.6 mm vertically. The depth of the hole was 2.8 ± 0.1 mm in each case. To retain the connection tightness, the glass tube was pasted with the cyan acrylic glue.

According to the instruction provided by the producer, the mixing process of the bone cement components was maintained until the solid consistency mass was achieved, which did not take longer than 60 s. In the first trial, the cement was mixed carefully, limiting the number of press movements to 12 cycles. In the next trial, the cement was mixed at the speed advised by the producer, 24 cycles per minute, and in the third trial the number of cycles increased up to 32. The bone cement was injected into the vertebral body models. The flow speed was set to 1.0 cm³/min on the infusion pump (assuming an incompressible medium). To minimize the temperature influence on the experiment, all the trials were carried out in the laboratory where the temperature was 24 ± 1°C. The cement flow was stopped in each trial when it started to flow out of the vertebrae model or when the entire volume of the prepared cement was administered. After the cement hardened, the samples were scanned with the CT scanner GE/LfC, with 0.074 mm definition. The reconstructed pictures of the vertebral bodies were used to evaluate the influence of aerification on the bone cement distribution in the specific models.

Results

The results were correlated and depicted in the pressure characteristics diagram as seen in FIG. 3. For every measurement, the time equal to 0 s referred to the beginning of the pump press movement.

There were characteristic points on each curve. The dashed vertical lines shown in the diagram corresponded to the moments when the cement crossed the feed channel and began to fill the vertebrae models. In all the cases, after filling the feed channel, there was the pressure increase resulting from the cement propagation in the stem model narrow channels (high local speed and increased resistance to movement). When the interior of the vertebrae model was filled with the reduced density, the pressure increase was lower. It can be concluded that this phenomenon was related to the vertebrae structure, whose thin structure in the center of the stem thickened towards the walls. As a result, the flow channels were narrower near the wall, resulting in the higher local velocity and the faster increase in pressure.

Despite the same flow rate set on the infusion pump, the course of the curves and the resulting cement delivery parameters differed on the case-by-case basis. The cement volume was also different. According to the indications of the infusion pump (for an incompressible fluid), the bone cement volume introduced through the system into the vertebral models was 7.0, 7.4, and 7.5 cm³, respectively. Using the CT data, the segmentation was performed and the bone cement volume inside the individual models was observed. The results are summarized in TABLE 1.
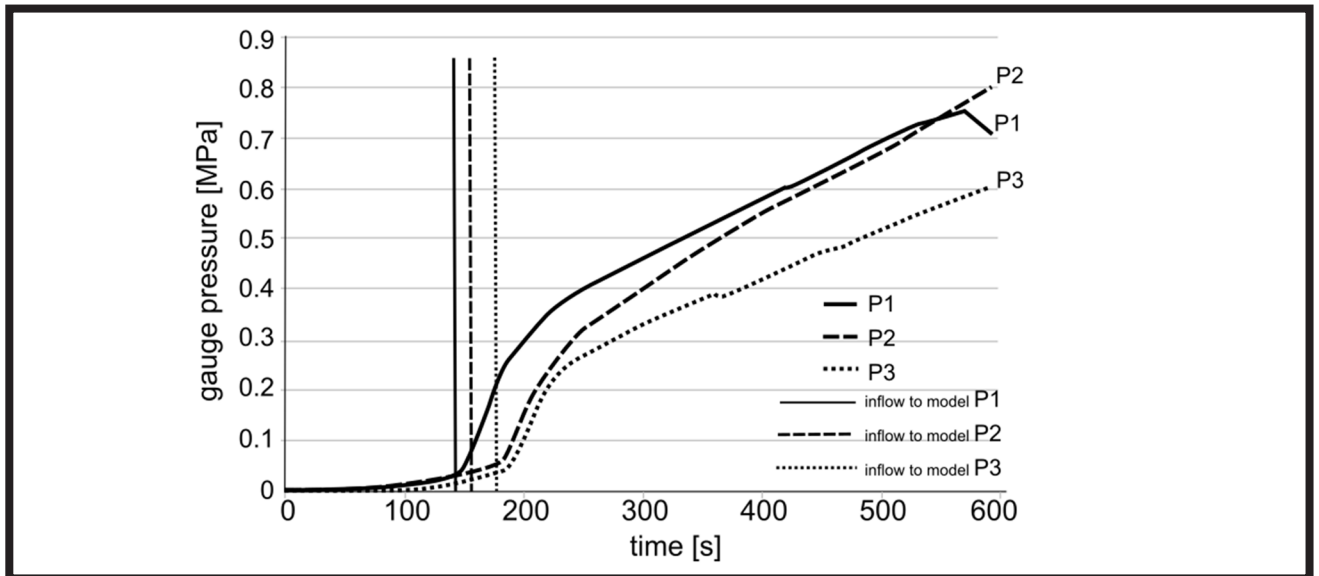
FIG. 3. Pressure characteristics acquired for every experimental case under analysis.

TABLE 1. Cement volume for vertebral bodies based on computer tomography.

Case	Total cement volume in the scanned sample [mm³]	Cement volume inside the vertebral body [mm³]
P1	5429.17	4602.41
P2	4877.17	4473.31
P3	2713.52	2525.62

Despite the same flow conditions and similar geometric conditions, the differences in the cement distribution can be seen in the CT scans (FIG. 4). In the first and second experiments, the cement filled the central space under the top border plate, the middle of the body and flowed into the left and right vertebral body walls. To some extent, it also filled the left side of the bottom body plate. In the third experiment, the cement filled the central space under the top boarder plate and the middle of the vertebral body. In the last case, the penetration had a much narrower range than in the previous two cases. In the third experiment, the cement did not fill the space above the top boarder plate. In every case, the cement tended to leak out through the anatomic foramen of the model back wall.

The transverse plane was used to provide the detailed distribution analysis for the five selected planes, according to the schemes presented in FIG. 5.

The results of the analysis were presented in a graphic form (FIG. 6) for the selected horizontal planes, every 4 mm, starting with the supply channel level to finish 3 mm below the boarder plate surface. The distribution in the central part surrounding the supply channel was rather regular for the 3 mm and 7 mm planes under the boarder plate. In the middle 11 mm plane, the medium flowed away in the direction of the anatomic foramen. For the 15 and 19 mm planes, the medium flowed into the front and the left body wall, which could be caused by the thinner vertebral body structure in this area.

In the microtomography images (FIG. 7) of the cross-section of the first sample P1, filled with the cement mixed with half the number of cycles, numerous air bubbles were observed. Air bubbles were found in the whole cement volume filling the vertebral body, as well as in the supply channel, where they clearly concentrated in its central area. In the second sample P2, filled with cement mixed with the number of cycles advised by the manufacturer, the quantity of air bubbles was lower in the vertebral body and in the supply channel. Air bubbles were smaller than those observed in the P1 sample. In the third sample P3, filled with the cement mixed with a higher number of cycles by half, large air bubbles were observed. The vertebral body filling was homogenous, and the cement filled numerous empty spaces in the body. There were longitudinal air bubbles in the cement in the supply channel.

Discussion

There were differences between the volume indications of the applied cement read from the infusion pump and the measurement results based on the TC scan. The reason for these differences was the fact that infusion pumps were to work with incompressible fluids, such as liquid medications, so they did not have a feedback loop. This phenomenon proved that the cement aerification should not be omitted during vertebroplasty procedures or while developing a mathematical model for the bone cement. Furthermore, the pump showed a given volume, although some cement was already lost to fill the supply channel.

The large number of small pores in the cement, especially in the cannula vicinity, showed that the cement could not be treated as a homogenous liquid. The high level of aerification may influence the cement further distribution. The numerous air bubbles in the flowing material may be constantly squeezed by pressure. As a result, the volume flow rate could significantly reduce in the further part of the channel.

All the above-mentioned differences (flow time, pressure characteristics, and a given volume) could stem from the three main factors: a random level of cement aerification, a difference in viscosity of the 3D printed models dependent on the printing time and precision. An influence of the temperature coming from a chemical reaction of cement with the 3D model structure should not be excluded either (glass transition temperature PLA 60-65°C).
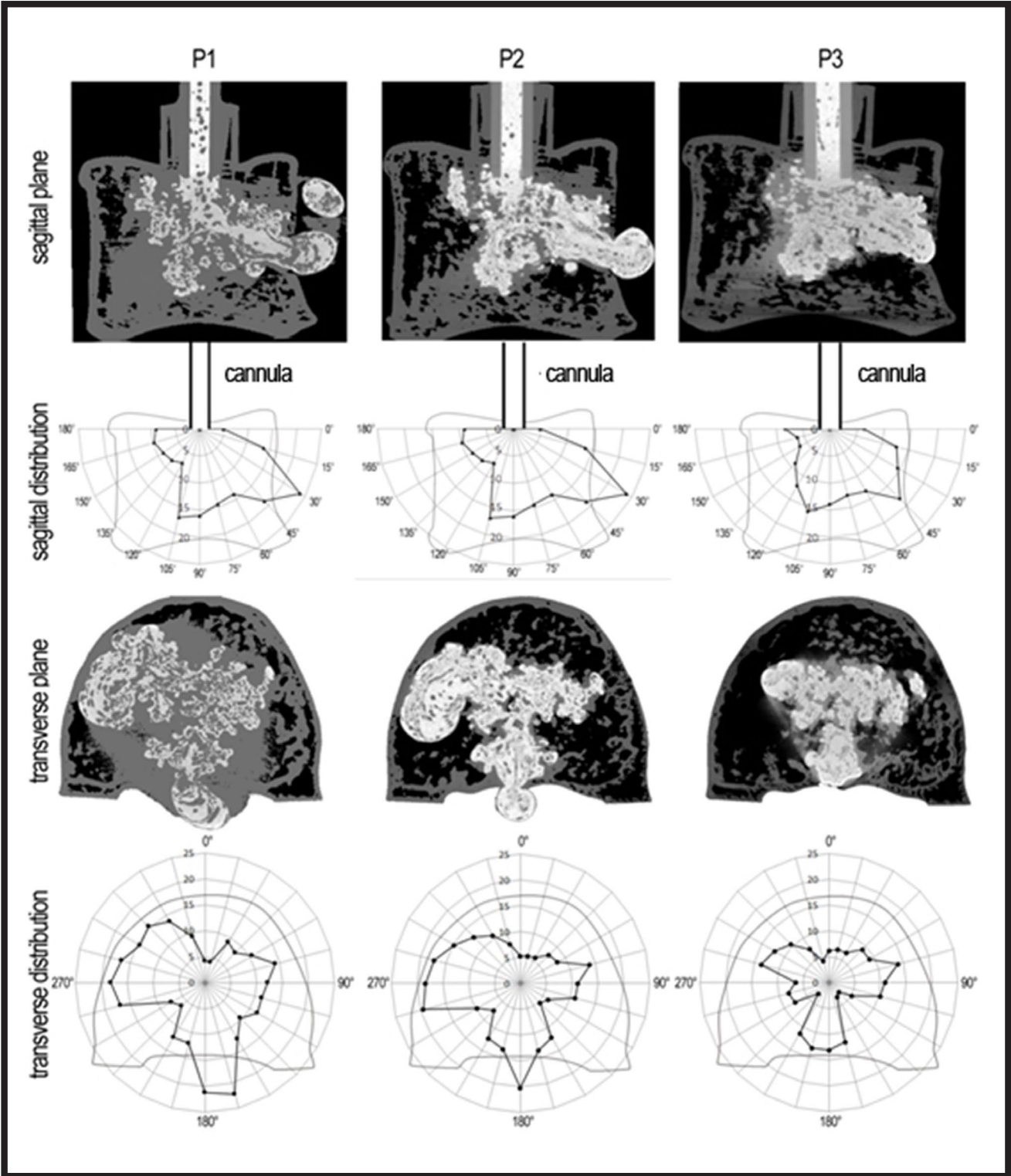
FIG. 4. Cement distribution in the sagittal plane through the vertebra center, and transverse plane for the middle slice (11 mm) of the vertebrae models for every case P1, P2 and P3 under analysis.
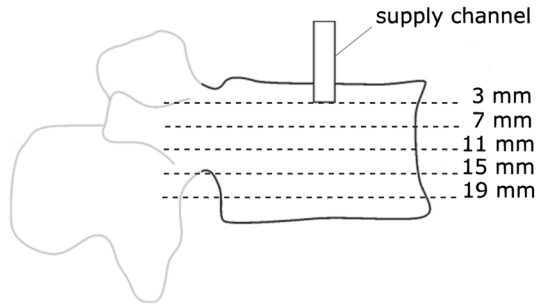
FIG. 5. Schematic view of the section position in the sagittal plane for evaluating the cement distribution.
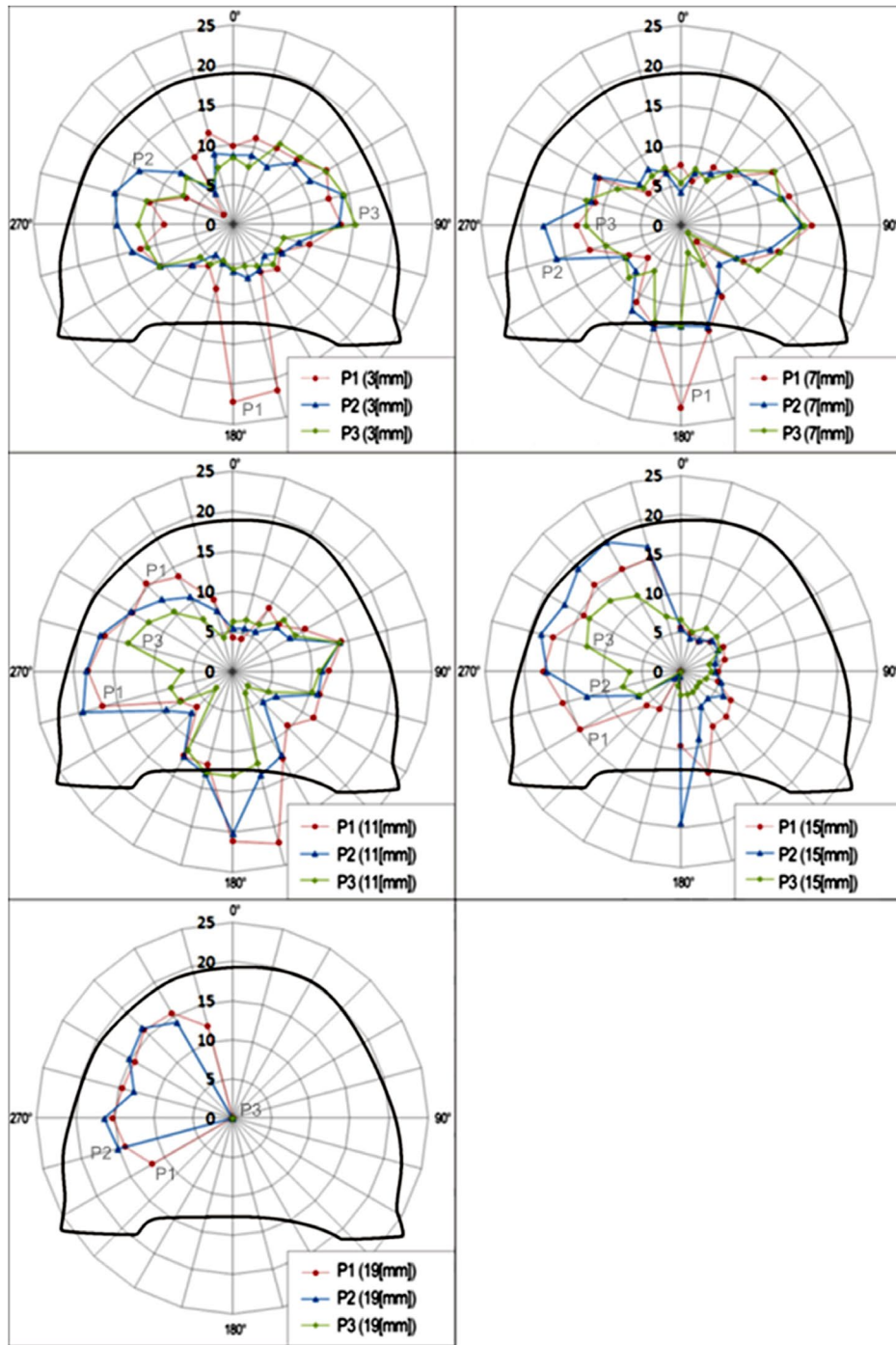
FIG. 6. Cement distribution in selected planes of the vertebral body models – the black contour.
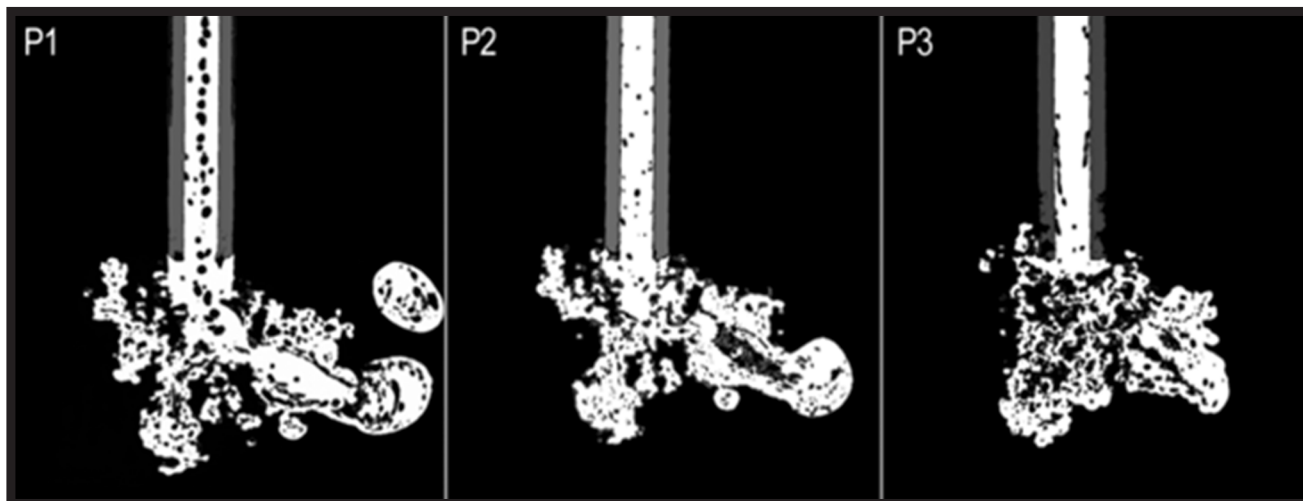
FIG. 7. Aerification of cement in the sagittal plane for every case under analysis.

Conclusions

The aerification level of bone cement had an important influence on the bone cement distribution in the vertebral body model. The low-aerified cement could penetrate well, which allowed the vertebral body to be filled evenly. The too high level of aerification lowered the penetration extent and influenced the homogeneity of the body being filled, which could influence its further biomechanical properties. The more precise interpretation requires further research in the field of aerification and the influence of its level on the medium distribution

The tested models proved the 3D printing technique useful in the preparation of anatomical vertebral body models. However, the question remains whether the FDM resolution is sufficient or the SLA technology would be a better solution. The three-dimensional vertebral body models used in the experiments are easily accessible and inexpensive in comparison to the man-made unconsolidated preparations which are limited. Additional body models can be quickly replicated, which will enable further experiments to be conducted under comparable conditions.

Acknowledgements

Declaration of Competing Interest
The authors declare that they have no known competing financial interests or personal relationships that could have appeared to influence the work reported in this paper.

ORCID iD

A. Bonik: https://orcid.org/0000-0002-6094-2425
Z. Tyfa: https://orcid.org/0000-0001-9870-8370
L. F. Ciupik: https://orcid.org/0000-0002-8830-6965
K. Sobczak: https://orcid.org/0000-0001-8994-6908
A. Kierzkowska: https://orcid.org/0000-0003-3800-2733
D. Obidowski: https://orcid.org/0000-0002-8950-6424
D. Witkowski: https://orcid.org/0000-0003-4804-0266
T. Pałczyński: https://orcid.org/0000-0002-2898-5302
M. Elgalal: https://orcid.org/0000-0001-9127-0169
P. Komorowski: https://orcid.org/0000-0002-4035-7501
E. Słoński: https://orcid.org/0000-0001-7379-0128
K. Jóźwik: https://orcid.org/0000-0002-7596-3691
B. Walkowiak: https://orcid.org/0000-0003-4867-5456

References

[1] Conference report. Consensus development conference: diagnosis, prophylaxis, and treatment of osteoporosis. The American Journal of Medicine 94 (1993) 646-650.

[2] Hsuan-You Chen, Yen-Po Lin, Han-YingWang, Feng-Huei Lin, Po-Quang Chen, Ding-cheng Chan, Tze-Hong Wong, Ming-Hsiao Hu: Safer way for vertebroplasty under fluid mechanics theory. The Spine Journal 20 (2020) S77-S135.

[3] Andrei D., Popa I., Brad S., Iancu A., Oprea M., Vasilian C., Poenaru D.V.: The variability of vertebral body volume and pain associated with osteoporotic vertebral fractures: conservative treatment versus percutaneous transpedicular vertebroplasty. International Orthopaedics 41 (2017) 963-968.

[4] Adams M.A., Dolan P.: Perspective: Spine biomechanics. Journal of Biomechanics 38 (2005) 1972-1983.

[5] Dengwei He, Chao Lou, Weiyang Yu, Kejun Zhu, Zhongwei Wu, Feijun Liu, Minjang Chen, Lin Zheng, Zhenzhoing Chen, Shunwu Fan: Cement distribution patterns are associated with recompression in cemented vertebrae after percutaneous vertebroplasty: a retrospective study. World Neurosurgery 120 (2018) e1-e7.

[6] Biancji E., Chiusa F., Pennati G.: Computational fluid dynamics of bone cement in procedures for osteoporosis treatment. 16th ESB Congress, Presentation, O154, S157.

[7] Huber G., Muller-Bergen L., Heinze J., Eggers C., Purschel K., Morlock M.M.: Mechanical stability of augmented spinal segments. 5th World Congress of Biomechanics, München (2006).

[8] Lin C-Y., Chuang S-Y., Ju D-T., Chen W-P.: Effects of bone stiffness, cement volumes and vertebral body height loss on the load transfer change of adjacent vertebrae in percutaneous vertebroplasty. Journal of Biomechanics 40 (2007) 584-585.

[9] Wang J-L., Chiang Ch-K., Kuo Y-W., Chou W-K., Yang B-D.: Mechanism of fractures of adjacent and augmented vertebral following simulated vertebroplasty. Journal of Biomechanics 45 (2012) 1372-1378.

[10] Jung Sik Bae, Heong Hyun Park, Ki Joon Kim, Hyeun Sung Kim, Il-Tae Jang: Analysis of risk factors for secondary new vertebral compression fracture following percutaneous vertebroplasty in patients with osteoporosis. World Neurosurgery 99 (2016) 387-394.

[11] Tschirhart C.E., Roth S.E., Whyne C.M.: Biomechanical assessment of stability in the metastatic spine following percutaneous vertebroplasty: effects of cement distribution patterns and volume. Journal of Biomechanics 38 (2005) 1582-1590.

[12] Tyfa Z., Witkowski D., Sobczak K., Obidowski D., Jóźwik K.: Experimental investigations of the aerated polymethylmethacrylate--based vertebral cement flow in capillaries. The International Journal of Artificial Organs 41(10) (2018) 670-676.

[13] Race A., Mann K.A., Edin A.A.: Mechanics of bone/PMMA composite structures: An in vitro study of human vertebrae. Journal of Biomechanics 40 (2007) 1002-1010.

[14] Tarsuslugil S.M., O'Hara R.M., Dunne N.J., Buchanan F.J., Orr J.F., Barton D.C., Wilcox R.K.: Development of calciumphosphate. Journal of Biomechanics 46 (2013) 711-715.

[15] Kinzl E., Boger A., Zysset P.K., Pahr D.H.: The effects of bone and pore volume fraction on the mechanical properties of PMMA-bone biopsies extracted from augmented vertebrae. Journal of Biomechanics 44 (2011) 2732-2736.

[16] Baroud G., Falk R., Crookshank M., Sponagel S., Steffen T.: Experimental and theoretical investigation of directional permeability of human vertebral cancellous bone for cement infiltration. Journal of Biomechanics 37 (2004) 189-196.

[17] Boger A., Wheeler K., Montali A., Gruskin E.: NMP-modified PMMA bone cement with adapted mechanical and hardening properties for the use in cancellous bone augmentation. Journal of Biomedical Materials Research Part B: Applied Biomaterials 90(2) (2009) 760-766.

[18] Kwon S.Y., Cho E.H., Kim S.S.: Preparation and characterization of bone cements incorporated with montmorillonite. Journal of Biomedical Materials Research Part B: Applied Biomaterials 83(1) (2007) 276-284.

[19] Arabmotlagh M., Rickert M., Lukas A., Rauschmann M., Fleege Ch.: Small Cavity Creation in the vertebral body reduces the rate of cement leakage during vertebroplasty. Journal of orthopaedic research 35(1) (2017) 154-159.

[20] Orlando O.A.: Vertebroplasty Cement Augmentation Technique. In: Razi A., Hershman S. (eds) Vertebral Compression Fractures in Osteoporotic and Pathologic Bone. Springer, Cham (2020) 115-135.

[21] Furtos G., Tomoaia-Cotisel M., Baldea B., Prejmerean C.: Development and characterization of new AR glass fiber reinforced cements with potential medical applications. J Appl Polym Sci, 128(2) (2013) 1266-1273.

[22] Furtos G., Tomoaia-Cotisel M., Garbo C., Şenilă M., Jumate N., Vida-Simiti I., Prejmerean C.: New composite bone cement based on hydroxyapatite and nanosilver. Particul Sci Technol 31(4) (2013) 392-398.

[23] Barakat A.S., Alhashash M., Shousha M., Boehm H.: What an orthopaedic surgeon should know about vertebral cement augmentation. Current Orthopaedic Practice 28(4) (2017) 409-416.

[24] Slane J., Vivanco J., Rose W., Ploeg H.L., Squire M.: Mechanical, material, and antimicrobial properties of acrylic bone cement impregnated with silver nanoparticles. Materials Science and Engineering: C48 (2015) 188-196.

[25] Farrar D.F., Rose J.: Rheological properties of PMMA bone cements during curing. Biomaterials 22(22) (2001) 3005-3013.

[26] Spierlings P.T.: Properties of bone cement: testing and performance of bone cements. The Well-Cemented Total Hip Arthroplasty: Theory and Practice. Heidelberg: Springer Medlizin Verlag Heidelberg (2005) 67-78.

[27] Hernández L., Gurruchaga M., Goñi I.: Influence of powder particle size distribution on complex viscosity and other properties of acrylic bone cement for vertebroplasty and kyphoplasty. Journal of Biomedical Materials Research, Part B: Applied Biomaterials 77(1) (2006) 98-103.

[28] Pietroń K., Mazurkiewicz Ł., Sybilski K., Małachowski J.: Correlation of Bone Material Model Using Voxel Mesh and Parametric Optimization. Materials 15(15) (2022) 5163.